

Reports

X-ray Pulsar in the Crab Nebula

Abstract. *X-ray pulsations have been observed in the Crab Nebula at a frequency closely matching the radio and optical pulsations. About 5 percent of the total x-ray power of the nebula appears in the pulsed component. The x-ray pulsations have the form of a main pulse and an interpulse separated by about 12 milliseconds.*

We wish to report the discovery of an x-ray pulsar in the general direction of the Crab Nebula. The data were obtained during an Aerobee rocket flight on 13 March 1969. Since the Crab Nebula is the only known x-ray source in that area and the period of the pulsar is identical with that of the radio and optical pulsar NP 0532, identification of the x-ray pulsar with that object appears certain.

Pulsars, radio-emitting "stars" having rapid and extremely accurately repetitive changes in luminosity with time, were discovered in 1968 by Hewish, Bell, Pilkington, Scott, and Collins (1). Staelin and Reifenstein (2) reported in late 1968 the discovery of two radio pulsars in the vicinity of the Crab Nebula, the optical remnant of a supernova explosion that occurred in A.D. 1054. These two are the longest-period (3.745 second) and shortest-period (33.09 msec) pulsars yet discovered.

In January of 1969, Cocke, Disney, and Taylor (3) reported the discovery of optical-light flashes from the Crab Nebula. The flashes occurred with the same period as the fast Crab pulsar (NP 0532) and were suggested as originating in the south-preceding of the two central stars in the Crab Nebula. This star, discussed by Minkowski (4), is very blue and exhibits a featureless spectrum. Using synchronous electronic photography, Miller and Wampler (5) at the Lick Observatory were able to demonstrate essentially complete disappearance of this star when their chopper was out of phase with the pulsations. At the time of this writing, the Crab pulsar is still the only one of some 30 pulsars for which the optical source has been identified.

The present measurement was made

from an Aerobee rocket, launched from White Sands Missile Range at 22:30 M.S.T. on 13 March 1969 (05:30 U.T., 14 March). The x-rays were detected with two proportional counters filled with 10 percent methane in argon at 800 mm-Hg pressure. One counter had a window of 3.8- μ -thick Mylar and an effective area of about 300 cm², while the other counter had a 3.2- μ -thick Teflon window and an effective area of about 250 cm². Each detector was fitted with a honeycomb-shaped collimator having a field of view of about 10°. The counters were continuously supplied with gas from reservoirs, and each counter system was internally stabilized against changes in the gas gain. The Mylar-window counter was sensitive (efficiency > 0.10) in the photon energy region 1 to 13 keV, with an additional narrow region near 0.25 keV; the Teflon-window counter was sensitive in the 1.2- to 13-keV region and also near 0.65 keV. Immediately before the Crab was observed, radioactive sources (Fe⁵⁵) were placed in front of the detectors for 10 seconds; this served as an energy calibration and as a random-noise reference for the pulsar analysis. An attitude control system (6) then pointed the x-ray detectors toward the Crab Nebula for 40 seconds. During this time the centers of the de-

tector fields of view, determined from aspect photographs, were always less than one degree from the Crab.

The individual pulses from each counter, minus the coincident counts from cosmic ray guard counters, were digitized and telemetered to the ground by a pulse-code-modulation system (7). Since the average total count rate from both detectors was about 2400 count/sec from the Crab, and the time required to transmit a pulse was about 20 μ sec, about 5 percent of the pulses was lost in the telemetry process. The digital pulses, when received on the ground, were stored on magnetic tape, along with a 200-khz reference frequency generated by a crystal-controlled clock at the ground station.

The first step in the search for a pulsar consisted in generating a computer-compatible tape from this digital tape. The number of counts that occurred in each 0.1-msec interval (judged by the 200-khz reference frequency) was recorded sequentially through the 40-second observation period. With the use of a computer, the data were then summed over 1.6-msec intervals. A power-spectrum analysis similar to that which we reported (8) for several other x-ray sources was performed, and part of the result is shown in Fig. 1. The power spectrum of the Fe⁵⁵ source is shown in the lower part of the figure. Bars signifying one-standard-deviation error, plus and minus, are plotted for every tenth point. The rise present at low frequencies is due to occasional timing errors on the record, which prohibited construction of a "light curve" from this particular tape. The upper portion of the figure is the power spectrum (square of the amplitude of the Fourier components in a specific frequency interval) for the first half (20 seconds) of the Crab observation. Peaks are present at 30.2 hz, which is the known fundamental frequency of NP 0532, and at several higher harmonics, as expected for a nonsinusoidal pulse. The highest frequency examined was 312.5 hz. Comparison of the power

Table 1. Characteristics of NP 0532.

	Radio (13)	Optical (3)	X-ray
Average pulsed power (erg cm ⁻² sec ⁻¹)	6×10^{-14} (195-430 Mhz)	8×10^{-12} (4500-8500 Å) U-B = -1.3*	1.5×10^{-9} (1-10 Å)
Spectral index	-2	B-V = +0.1	~0.4
Separation of main pulse and interpulse	~14.5 msec	14.0 msec	~12.0 msec
Half-power width of main pulse	~3.0 msec	1.4 msec	~2.5 msec
Half-power width of interpulse		3.0 msec	~5.0 msec

* U, B, and V are logarithmic intensities (magnitudes) in the ultraviolet, blue, and visual, respectively.

spectrum of the first half of the Crab data with that for the last half shows no significant peaks at frequencies other than harmonics of 30.2 hz, and no correspondence of marginally significant peaks in the two halves of the data. We can conclude, therefore, that no additional x-ray pulsar is present in the vicinity of the Crab Nebula having a pulsed component, in the frequency range 10 to 300 hz, greater than 2 percent of the total x-rays from the Crab.

After finding pulsations at a fre-

quency near that of the radio and optical pulsar, we constructed a "light curve," or phase diagram (Fig. 2), by superimposing many periods of the pulsar. The points shown in Fig. 2 were obtained by decoding the pulses on the digital magnetic tape and storing them in a multichannel analyzer, its multiscaler mode being used. The channels were advanced at the rate of 0.4 msec per channel, so that the pulsar period covered about 83 channels of the memory. The multiscaling continued to 128

channels, where the accumulation stopped until a gate pulse caused another pass to begin in synchronization with the pulsar period. This gate pulse was generated by counting the 200-khz reference frequency for 6619 cycles repeatedly, corresponding to a pulsar period of 33.095 msec. In Fig. 2, the channels have been added in discrete groups of two.

Although the x-ray points in Fig. 2 show a double pulse structure rather similar to the optical data (dashed line) of Nather *et al.* (3), caution must be exercised in interpreting the structure of the x-ray "light curve." The period was specified to an accuracy of one part in 6619, and the total number of periods examined was about 1200. The pulsations, therefore, could have been widened by as much as 18 percent of the period, or about 6 msec; that the main pulse was less than half this value is fortuitous. We calculate a period (for 13 March) from the optical observations (3) of 33.0967 msec, which differs from 33.095 by just less than half the precision in the latter. Our observations, then, are consistent with a period identical in the optical and x-ray regions, to slightly more than four significant figures. Since part or all of the 2.5-msec half-width of the main pulse may be due to phase mismatch, no structures finer than this are certain. Further analysis with a vernier adjustment of the period may reveal some structural features of the pulsations.

The interpulse of the x-ray data has a lower peak and is about twice as wide as the main pulse; in these features it resembles the optical pulsar. However, the x-ray interpulse actually contains more counts than the main

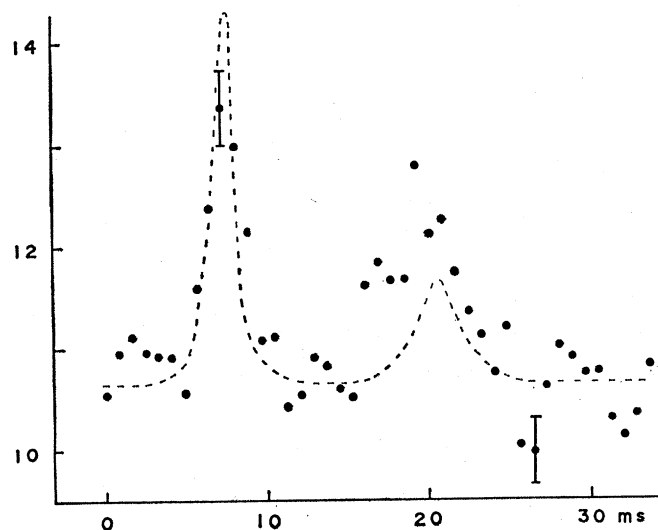
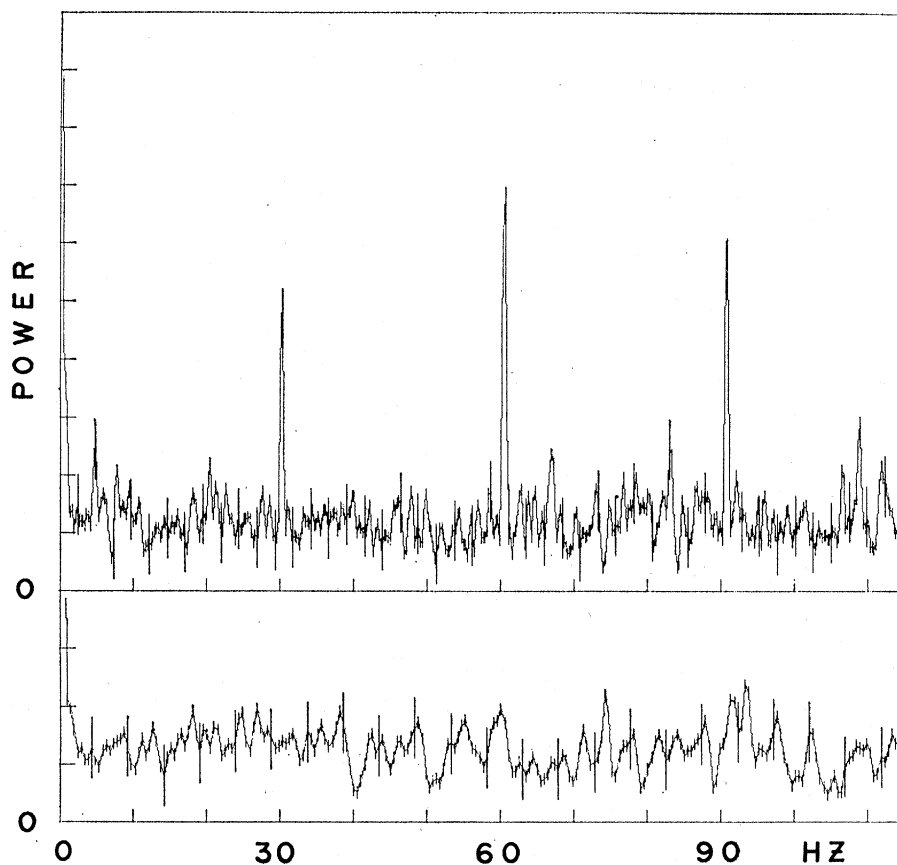


Fig. 1 (above). Power spectra derived from observations of x-rays from 3 to 15 Å, from the Crab Nebula (top) and from an Fe^{55} source observed just previously. Relative power (which is proportional to the square of the amplitude in a frequency interval) is plotted (on a linear scale) against the frequency in hertz. The radio and optical Crab Nebula pulsar is known to have a frequency of 30.2 hz, which coincides with the x-ray pulse frequency. The power peaks repeat at higher harmonics of the fundamental frequency. Fig. 2. (left). The "light curve" (intensity as a function of phase) for the Crab Nebula x-ray pulsar (dots). The vertical scale is hundreds of counts per 0.8-msec phase interval. Error bars indicate plus and minus one standard deviation. Phase is in milliseconds. The dashed line is the optical pulsar adjusted so that the higher x-ray and optical peaks coincide in phase. The vertical scale on the optical pulsar has been adjusted to provide best agreement with the x-ray data, solely to facilitate relative phase comparisons.

pulse, and its onset is earlier than the optical counterpart. Whether these are significant permanent features or merely reflect time-variability in the pulsar will only be determined when simultaneous optical and x-ray measurements are made. The relative phase of the optical and x-ray data shown in Fig. 2 is arbitrary; the peaks are superimposed simply to illustrate the relative similarities.

The x-ray pulsed flux amounts to about 5 percent of the integrated x-ray flux of the entire nebula (3 to 15 Å). If the total x-ray flux (1 to 10 Å) of the Crab is about 3×10^{-8} erg cm $^{-2}$ sec $^{-1}$, then the corresponding x-ray pulsar flux is 1.5×10^{-9} erg cm $^{-2}$ sec $^{-1}$. Furthermore, the pulsar x-ray power is about 200 times the optical power and about 2×10^4 times the radio power.

In 1964, the Naval Research Laboratory (NRL) group observed a lunar occultation of the x-ray emission of the Crab (9). From the gradual decrease of x-ray flux during the covering of the nebula, it was determined that the x-ray emission was nebular rather than stellar. Within the statistical accuracy of the observations a stellar contribution as great as 5 percent could not have been detected.

The Crab Nebula was first identified as a soft x-ray source (2 to 8 Å) by the NRL group (10) in 1963 and subsequently has been observed up to 500 keV (11). Figure 3 (segments E-I) shows the spectral shape from 10^7 to 10^{20} Hz (3, 12, 13). Overall this broad range, the nebular radiation is believed to be synchrotron in origin. The x-ray flux from 2 to 500 keV can be attributed to an inverse power law distribution of relativistic electrons

$$N(E) dE \sim E^{-2.2} dE$$

Electrons with energies of about 10^{13} to 10^{14} eV gyrating in a field of about 5×10^{-4} gauss are required to account for the observed x-rays. The electrons cannot survive more than a few years to a few months, depending on the energy.

Figure 3 also shows (segments B-D) the shape of the pulsed radiation spectrum of the Crab. Included (segment A) is the low-frequency spectrum of the point source first discovered by Hewish and Okoye (14). The dimension of this source, determined from scintillation measurements, is less than 0.1 sec of arc ($\sim 3 \times 10^{15}$ cm at 2 kparsec). Rees (15) has attributed the emission to proton-synchrotron radiation, which

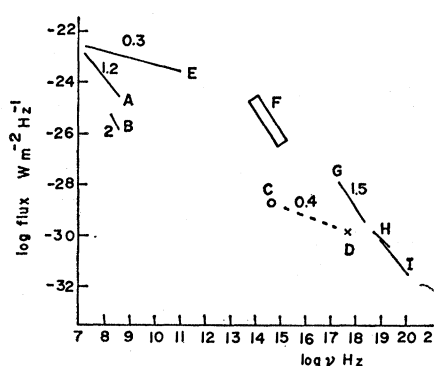


Fig. 3. Spectrum of the Crab Nebula and pulsar NP 0532. The logarithm of the flux is plotted against the logarithm of the electromagnetic frequency. Some lines are labeled with negative slopes (spectral index). A represents the small radio source in the Crab, which may be associated with the pulsar. B is the radio pulsar, C the optical pulsar, and D the present x-ray pulsar observation, which is plotted relative to G, the x-ray spectrum of the entire nebula as determined by other workers. H and I are higher energy spectra of the Crab (as a whole), while E and F are similar spectra in the radio and optical regions, respectively.

requires energies of ~ 30 GeV in a magnetic field of ~ 50 gauss. The fact that the spectral indices of both the low-frequency point source and the radio pulsar are considerably larger than that of the general nebular radio emission strongly suggests that both concentrated sources have a common origin. Although the optical flux is indicated in Fig. 3 by a point, sufficient evidence already exists to indicate that the optical spectrum is comparatively flat (3). The spectrum of optical pulsations does not appear to be related to the radio pulsations in the simple way that all of the nebular radiation can be attributed to electron synchrotron radiation. If the optical and x-ray pulsed fluxes are joined by a straight line, as a preliminary spectral analysis of the pulsed x-rays suggests may be appropriate, the slope is only 0.4 compared to about 1.5 for the nebular soft x-ray emission.

It is generally believed that pulsars are neutron stars and that the pulsar period is associated with the spin period (16, 17). In the collapse to the neutron star configuration, the stellar magnetic field may be greatly amplified at the surface and may form a magnetosphere about the star. Gold (16) has proposed that plasma locked in rotation with the magnetosphere reaches relativistic velocities and is expelled into the nebula. The observed decreasing spin frequency of NP 0532 implies

a dissipation of 10^{38} erg/sec of kinetic energy of rotation which, if efficiently converted to relativistic plasma, could supply all the observed synchrotron radiation. Other models, such as the eccentric magnetic dipole of Gunn and Ostriker (17), also obtain the pulsed radiation from the rotational energy.

The shape of the pulsar spectrum suggests that the radio emission mechanism differs from that producing the optical and x-ray pulsations. Extending Rees's interpretation to the low-frequency pulsed radiation we may assume a proton-synchrotron process operating at distances from the stellar surface where the magnetic field is of the order of several hundred gauss. The optical and x-ray emission may be electron-synchrotron radiation, generated by relativistic electrons in comparable or stronger fields. If the pulsed energetic electrons are decoupled from the stellar rotation (Gold's model) in a magnetic field which is rapidly diverging outward from the star, the pulsed energy would be concentrated toward the x-ray region, so as to produce a much flatter spectrum than is observed in the nebula. It is clearly important to search for the pulsar, from balloon altitudes, at energies in the 10- to 100-keV range.

G. FRITZ
R. C. HENRY
J. F. MEEKINS
T. A. CHUBB
H. FRIEDMAN

*E. O. Hulburt Center for Space
Research, Naval Research Laboratory,
Washington, D.C. 20390*

References and Notes

1. A. Hewish, S. J. Bell, J. D. H. Pilkington, P. F. Scott, R. A. Collins, *Nature* **217**, 709 (1968).
2. D. H. Staelin and E. C. Reifenstein, *Science* **162**, 1481 (1968).
3. W. J. Cocke, M. J. Disney, D. J. Tavlör, *Nature* **221**, 525 (1969); also R. E. Nather, B. Warner, M. MacFarlane, *ibid.*, p. 527.
4. R. Minkowski, *Stars and Stellar Systems VII* (Univ. of Chicago Press, Chicago, 1968), p. 639.
5. J. S. Miller and E. J. Wampler, *Nature* **221**, 1037 (1969); see also *Sky and Telescope* **37**, 231 (1969).
6. Supplied by Aerojet-General Corporation. We thank J. La Buda and M. Watson for the excellent performance of this vital component.
7. Designed and built by the Physical Sciences Laboratory, New Mexico State University.
8. H. Friedman, G. Fritz, R. C. Henry, J. P. Hollinger, J. F. Meekins, D. Sadeh, *Nature* **221**, 345 (1969).
9. S. Bowyer, E. T. Byram, T. A. Chubb, H. Friedman, *Science* **146**, 912 (1964).
10. —, *Nature* **201**, 1307 (1967).
11. R. C. Haymes, D. V. Ellis, G. J. Fishman, J. D. Kurfess, W. H. Tucker, *Astrophys. J.* **151**, L9 (1968).
12. Our Fig. 3 is adapted from a figure by E. P. Ney and W. A. Stein, *Astrophys. J.* **152**, L21 (1968), where detailed references are given.
13. J. M. Comella, H. A. Craft, Jr., R. V. E. Lovelace, J. M. Sutton, *Nature* **221**, 453 (1969).

14. A. Hewish and S. Okoye, *ibid.* **203**, 171 (1964); *ibid.* **207**, 59 (1965); see also I. S. Shklovsky, *Supernovae* (Wiley, New York, 1968), p. 248.
15. M. J. Rees, *Astrophys. Lett.* **2**, 1 (1968).
16. T. Gold, *Nature* **221**, 25 (1969).
17. J. E. Gunn and J. P. Ostriker, *ibid.*, p. 454.
18. This work was partially supported by NASA grant R-09-029-063; R.C.H. was supported by NSF grant GP-11855. The rocket vehicle and

vehicle support services were provided by the Sounding Rocket Branch, Goddard Space Flight Center; funding for the attitude control system was provided by NASA. We thank G. Kraft of NASA for directing the preparation of the launch vehicle. We thank D. P. McNutt for advice regarding computer treatment of rocket data tapes.

25 April 1969

Infrared Scanning Images: An Archeological Application

Abstract. Aerial infrared scanner images of an area near the Little Colorado River in north-central Arizona disclosed the existence of scattered clusters of parallel linear features in the ashfall area of Sunset Crater. The features are not obvious in conventional aerial photographs, and only one cluster could be recognized on the ground. Soil and pollen analyses reveal that they are prehistoric agricultural plots.

Thermal infrared scanning images of the eastern part of the San Francisco volcanic field about 40 km northeast of Flagstaff, Arizona, were recorded with a Reconofax IV (H.R.B. Singer Co.) infrared scanning radiometer in April, 1966. The radiometer was operated in the 8- to 14-micron region of the spectrum, and flight altitude

was 762 m above the ground surface.

The images revealed the presence of linear features which subsequent investigations showed bordered previous unrecognized prehistoric agricultural plots (Fig. 1a). The plots are barely visible on black and white aerial photographs (Fig. 2) that were obtained at the same time as the infrared

images. Only one of the plots could be recognized by inspection on the ground (Fig. 1d).

The agricultural plots are in soil developed in basaltic ash and cinders overlying an upper Pliocene basalt flow. The one cluster of parallel rows recognized on the ground (Fig. 1d) consists of parallel ridges of fresh, gray-black, basaltic ash (mean size, 1 mm) alternating with subdued troughs in buff soil derived from weathering of the underlying basaltic cinders and ash. At present, both the ash ridges and intervening soil bands range from 3 to 4 m in width; the present relief of the ash ridges ranges from 5 to 30 cm.

The ash ridges are visibly enhanced [white bands (Fig. 1)] on the infrared images as a result of their lower thermal inertia and relatively higher radiant temperatures during daylight hours (4:00 p.m.). Additional enhancement may have resulted from the slightly denser growth of Upper Sonoran desert grass (tentatively identified as *Bouteloua eriopoda*) on this dark ash unit.

Several kinds of evidence indicate

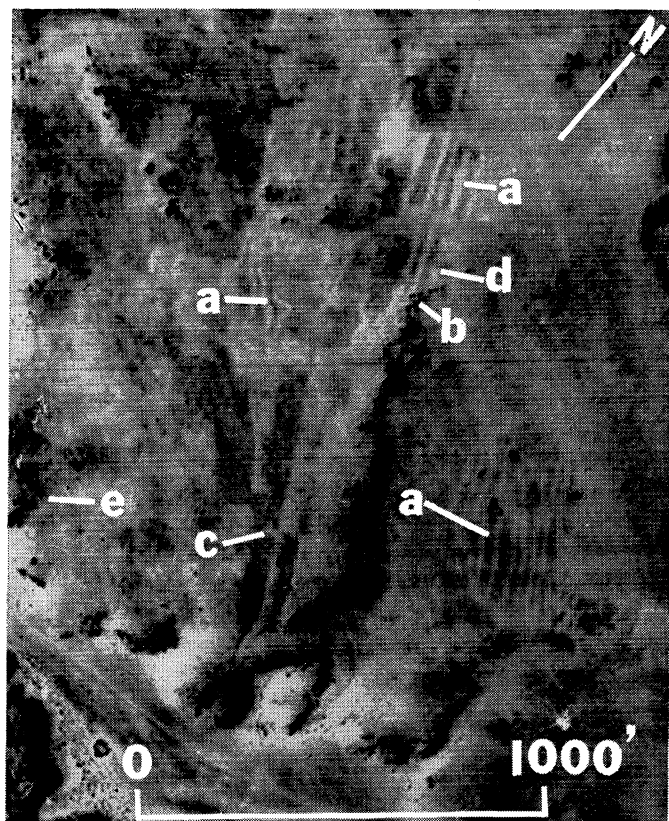


Fig. 1. Infrared scanner image of prehistoric agricultural plots. (a) Areas of agricultural activity; (b) prehistoric habitation sites; (c) wider than normal agricultural plot not recognizable on aerial photograph (Fig. 2); (d) area of soil samples 1 and 2; and (e) area of soil sample 3 (see Table 1).

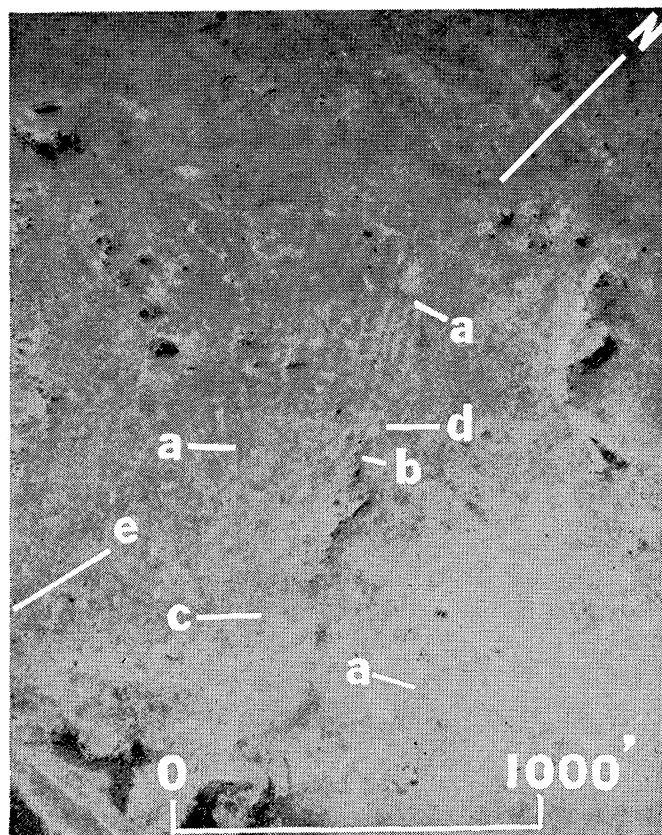


Fig. 2. Aerial photograph (Plus-X) of agricultural plots taken simultaneously with infrared image. (a) Areas of agricultural activity; (b) prehistoric habitation site; (c) region of unique wide farming plots (see Fig. 1). See Fig. 1 for explanation of (d) and (e).